International Journal of Science Academic Research
Vol. 06, Issue 10, pp.10798-10806, October 2025
Available online at http://www.scienceijsar.com

ISSN: 2582-6425

Research Article

ADSORPTION OF RHODAMINE B DYE FROM AQUEOUS SOLUTION USING AN ECO-FRIENDLY BIOSORBENT FROM MUSA PARADISIACA PEELS: EQUILIBRIUM AND KINETICS STUDIES

Kifline MILEBUDI KIFUANI, Grace Grace DIASONGA, *Anatole KIA MAYEKO KIFUANI, Bernick WEMBOLOWA TSHENE, Pitchou BOKOLOMBE NGOY, Gracien EKOKO BAKAMBO, Josaphat NDELO-DI-PHANZU and Daniel WA MUANDA MUKANA

Laboratory of Physical Organic Chemistry, Water and Environment, Department of Chemistry and Industry, Faculty of Sciences and Technology, University of Kinshasa, P.O. Box 190 Kinshasa XI, Democratic Republic of Congo

Received 14th August 2025; **Accepted** 17th September 2025; **Published online** 30th October 2025

Abstract

The eco-friendly biosorbent derived from *Musa paradisiacal* (MPB) was assessed for its capacity to adsorb Rhodamine B (RhB) from aqueous media. To achieve this, the influence of key operational parameters-including biosorbent mass, contact time, initial dye concentration, and solution pH-was systematically investigated.Adsorption was carried out in batch tests. After adsorption the supernatant was analysed by UV-Vis spectrophotometry to determine the residual concentration of the RhB solution.Adsorption modeling was done with the surface reaction kinetic model and Langmuir and Freundlich equilibrium models. The obtained results showed that MPB has a pH_{ZPC} of 5.51, a specific surface area of 292.52 m^2 g^{-1} and a maximum observed capacity (Q_{mo}) of 90.00 mg g^{-1}. The results demonstrated that the adsorption capacity of MPB increases with time and initial dye concentration, confirming a time-dependent uptake mechanism. Interestingly, the adsorption was only slightly influenced by pH, suggesting that electrostatic interactions are not the dominant driving force, and that other mechanisms such as hydrophobic interactions or specific binding sites may be involved. The optimal operating pH was determined to be 5.50, with a maximum adsorption capacity (Q_m) of 4.97 mg/g and a peak adsorption percentage of 79.48%.Kinetic modeling revealed that the pseudo-second-order model (R_g^2 = 0.9002) provided a better fit than the pseudo-first-order model (R_g^2 = 0.8975), indicating that chemisorption likely governs the adsorption process. Equilibrium data were best described by the Freundlich isotherm (R_g^2 = 0.9384), compared to the Langmuir model (R_g^2 = 0.9049), suggesting heterogeneous surface adsorption and the possibility of multilayer coverage. Overall, MPB proved to be an effective and stable biosorbent for Rhodamine B removal under varied conditions. Its compatibility with the pseudo-second-order kinetic model and Freundlich isotherm reinforces its potential for practical applications in wastewater treatment.

Keywords: *Musa paradisiaca*, Rhodamine B, Adsorption, Biosorbent, Kinetic, Equilibrium, Isotherm.

INTRODUCTION

Organic dyes are widely used in different industries for dyeing paper, textiles and other objects. In most cases industrial wastewater is discharged into the environment without prior treatment. Thus nearly 15 to 25% of organic dyes are found in wastewater, polluting, by vertical or horizontal migration, groundwater, aquifers and surface water (Narayana *et al*., 2019; Basma *et al*., 2024; Kifuani *et al*., 2024). They are likely to cause poisoning, cancer and respiratory pain in humans. Rhodamine B (RhB) is a synthetic xanthene dye used in scientific and industrial applications, such as printing and dyeing in paper, paints, inks, textiles, leathers, etc. It serves as a fluorescent tracer in biochemical assays, flow cytometry, and microscopy due to its strong fluorescence. Despite regulatory restrictions, Rhodamine B has also been found in some cosmetic and food products, particularly in regions where oversight is limited. Rhodamine B dye can cause serious environmental and sanitary problems, like irritation of skin, eyes and respiratory tract. The carcinogenicity, reproductive and developmental toxicity, neurotoxicity and chronic toxicity towards humans and animals have been experimentally proven (Jain *et al*., 2007; Cladelaud *et al*., 2023; Nyakairu *et al*., 2024).

Corresponding Author:** ***Anatole KIA MAYEKO KIFUANI,
Laboratory of Physical Organic Chemistry, Water and Environment, Department of Chemistry and Industry, Faculty of Sciences and Technology, University of Kinshasa, P.O. Box 190 Kinshasa XI, Democratic Republic of Congo

Rhodamine B is chemically stable and resistant to biodegradation, allowing it to persist in aquatic environments when discharged through industrial effluents. It poses risks to aquatic life due to its toxicity and potential to bioaccumulate. Its presence in water bodies not only threatens ecosystems but also complicates water treatment processes, making its removal a priority in environmental management. The removal of Rhodamine B and other organic dyes or inorganic pollutants from wastewater is therefore necessary. Several methods and techniques are used for the removal of Rhodamine B or other organic dyes from wastewater. These biological, chemical, or physical methods include the following techniques: adsorption, advanced oxidation, chemical and electrochemical oxidation, coagulation, flocculation, Fenton electron process, microbial and fungal decolorization, photocatalysis, nanofiltration, ozonation, reverse osmosis (Achouri *et al*., 2018; Hatiya *et al*., 2022; Gani *et al*., 2023). Of all these techniques, adsorption has proven to be a very effective technique. Activated carbon is the most widely adsorbent used for water treatment. But for the treatment of wastewater, its high production cost and its difficult regeneration make its use expensive (Jan *et al*., 2022; Hajir *et al*., 2024).For several years, biomass from agricultural waste has been tested as biosorbents for the elimination of organic dyes from water. These wastes include apricot stones, banana pith, coconut coir dust, cotton stalk, hazelnut shell, coffee residue, coir pith stone, green pea peels, groundnut shells, mango leaves, mango seed kernel, oil palm shell, orange peel, peach stones, sugarcane bagasse, sunflower stalks, yellow passion fruit waste, *Curcumeropsis manni* shells,

Manihot esculenta kernels (Kifuani *et al*.,2 018a; Jia *et al*., 2018; Ali *et al*,, 2021; Razia *et al*. , 2022;Ajala *et al*., 2024; Tshene *et al*., 2024; Mateso *et al*, 2025). These materials contain organic substances such us polyphenols, lignin, tannins, flavonoids, cellulose, starch, proteins, which provide active surface functions, such as carboxylic acid, ketone, aldehyde, phenol, lactone, pyrone, responsible for the adsorption of organic dyes or other pollutants on their surface (Razia *et al*., 2022; Kifuani *et al*., 2024). In this study the biosorbent from *Musa paradisiaca* (plantains banana) peels was used to eliminate Rhodamine B from systematically polluted water. Several adsorption parameters were studied including dose of adsorbent, contact time, initial concentration and pH of Rhodamine B solution.

MATERIALS AND METHODS

Biosorbent preparation

The biosorbent used was prepared using plantain peelings collected in Mbanza Ngungu, in Kongo Central province, in the Democratic Republic of Congo. The biomass was first dried in the sun and then in an oven at 105°C (DESPATCH Oven Co., type Elect) to eliminate of the water content. It was then crushed and sifted to obtain powder with particle size ≤ 500 um. The *Musa paradisiaca* biosorbent (MPB) thus obtained was stored in airtight packaging and placed in a desiccator at laboratory temperature (28°C), to keep it free from moisture contact and oxidation (Kifuani *et al*., 2018a).

Adsorbent characterization

Physicochemical parameters of the biosorbent (MPB) were determined including grain diameter, humidity, dry matter, ash content, pH of zero point of charge, specific surface area and maximum observed capacity.

Grain diameter

The diameter of the grains was determined by sifting using a sieve.

Humidity and dry matter

Volatilization gravimetry method was used to determine humidity (H) and dry matter (DM). For this purpose, 5 g of biosorbent were heated in an oven for 48 hours, after that the residual was waited. The humidity level (%H)of the biosorbent is then given by equation 1(Ajala *et al*., 2024).

$$\%H = \frac{(m_1 - m_2) \cdot 100}{m_1} \quad [1]$$

Where, m_1 and m_2, the weights of biosorbent before and after steaming, respectively.

The dry matter level (%DM) is calculated after deduction of the water content from 100% of the initial sample.

Ash content

Ash content of the biosorbent was determined by calcination 5 g of sample in a muffle furnace at 600°C (NABER, model N7 H) for 8 hours to obtain the ash. The ash content (%A) was calculated using the following equation 2 (Basma *et al*., 2024).

$$\%A = \frac{(m_3 - m_4) \cdot 100}{m_3} \quad [2]$$

Where, m_3 and m_4 being the weights of biosorbent before and after calcination, respectively.

Determination of pH_{ZPC}

The pH_{ZPC} (pH of zero point of charge) was determined by Boehm method or pH drift method. For this purpose, 100 mL of 0.01 mol L^{-1} NaCl solutions are placed in different Adsorbers (LACOPE ADX), and the pH of these solutions is adjusted from 2 to 12, by addition of 0.1 N HCl or 0.1 N NaOH solutions, to adjust the acidic or basic solutions, respectively. 1000 mg of biosorbent were then added to each solution and the suspension was stirred for 72 h, and centrifuged at 3000 rpm (Centrifuge Labofuge 200 Heraeus). The final pH of each solution was determined using a pH-meter (Hanna Instruments). The point of intersection of the curve obtained by plotting the final pH as a function of the initial pH of each solution determines the pH_{ZPC} (Kifuani *et al*., 2012; Musah *et al*., 2020).

Determination of the maximum observed capacity (Q_{mo}) and specific surface area (S_{MB})

The specific surface area of the biosorbent was determined by adsorption of methylene blue using the Kifuani volume variation method (KVVM). This method consists of studying adsorption of methylene blue, at equilibrium time, using a low mass of adsorbent. For this purpose, to 5 mg of adsorbent, increasing volumes (100 mL to 1000 mL) of the MB solution 50 mg/L are added. The suspension is stirred at the equilibrium time previously determined experimentally. The determination of the residual concentration of the supernatant by UV-spectrophotometry makes it possible to calculate the maximum adsorption capacity (Q_m) and the maximum adsorption capacity ($\%_m Ads$), using equations 3 to 5. The curve obtained by plotting the maximum adsorption capacity (Q_m) as a function of the volume (V) of the MB solution, makes it possible to determine the true maximum adsorption capacity, which we call maximum observed adsorption capacity (Q_{mo}); the others being apparent maximum capacities (Q_m). The maximum observed adsorption capacity is given by the plateau of this curve (Kifuani *et al*., 2012; Kifuani, 2013; Kifuani *et al*., 2018a).

$$A = \varepsilon . l . C \quad [3]$$

With, A being the absorbance, ε the molar absorption coefficient (L mg^{-1} cm^{-1}), l the thickness of the cell (1 cm) and C, the concentration of the solute (mg L^{-1}).

$$Q_m = \frac{(C_o - C_e)V}{m_B} \quad [4]$$

$$\%_m Ads = \frac{C_o - C_e}{C_o} \times 100 \quad [5]$$

With, Q_m being the maximum adsorption capacity of the biosorbent (mg g^{-1}), C_o the initial concentration of methylene blue solution (mg L^{-1}), C_e the residual or equilibrium concentration (mg L^{-1}), V the volume of the methylene blue solution (L),m_B the weight of the biosorbent and $\%_m Ads$, the maximum observed adsorption percentage.

The specific surface area (S_{MB}) is then calculated according to the following equation 6 (Kifuani *et al*., 2012):

$$S_{MB} = Q_{mo} \cdot N_A \cdot s \quad [6]$$

Where, S_{MB} being the specific surface area determined using MB as adsorbate (m^2 g^{-1}), Q_{mo} the maximum observed adsorption capacity (mg g^{-1}), N_A the Avogadro number (6.022 10^{23} mol^{-1}) and s, the area occupied by a MB molecule (175 $Å^2$).

Adsorbate and adsorbate solutions

Rhodamine B, a cationicdye, was used in this study as a model of organic toxic dye. His IUPAC name is 9-(2-carboxyphenyl)-6-(diethylamino)-N,N-diethyl-3H-xanthen-3-iminium chloride. Other names include Rhodamine 610, Basic violet 10, etc. Its chemical formula is $C_{28}H_{31}N_2O_3Cl$, Mw 479.01 g mol^{-1} and CAS number: 81-88-9.Its solubility in water is 50 g L^{-1}at 20°C. Figure 1 gives the structure of Rhodamine B. Rhodamine B used in this study was obtained from Merck and used without purification. All reagents used in this study were of analytical grade.

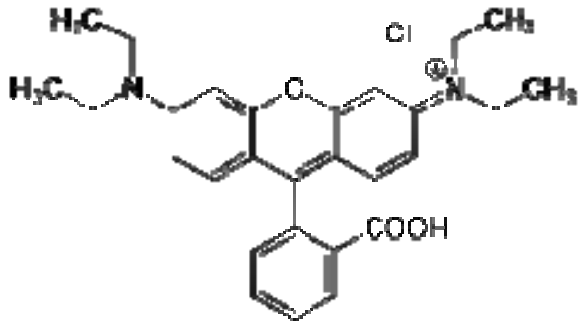

Figure 1. Structure of Rhodamine B

The preparation of Rhodamine Bsolutions was madeby dissolving RhB crystals in distilled water and diluting the resulting solution to obtain solutions ranging from 1mg L^{-1} to 100 mg L^{-1}. The pH of the RhB solutions was adjusted by adding 0.1 N HCl or 0.1 N NaOH solutions to obtain solutions ranging from pH 2 to 12. TheRhB solutions, before and after adsorption, were analyzed using a UV-Vis spectrophotometer (HACK Spectrophotometer, SP, model 1105) at maximum length wave determined experimentally, for each pH. The residual concentration of Rhodamine B solution was calculated using Beer-Lambert equation (equation 3) (Raiyyaan *et al*., 2021).

Batch adsorption experiments

The adsorption tests were carried out in batch experiment with adsorbers (LACOPE ADS) using 100 mL of RhB solution. Different parameters were studied, including mass of biosorbent MPB (1 mg to 1000 mg), contact time (0 to 400 minutes), concentration (10 mg L^{-1} to 100 mg L^{-1}) and pH (2 to12) of the RhB solution. Before use, the biosorbent was dried in an oven at 105°C for 3 h and the mass of the biosorbent was determined by weighting, using an analytical balance (HEB-E 303). After stirring for the required time, the suspension was centrifuged at 3000 rpm for 30 minutes and the supernatant was analyzed with a UV-Vis spectrophotometer at the appropriate wavelength, to determine the residual concentration of RhB solution. Each experiment is repeated three times to determine the absolute error. All the results were obtained with a confidence level ≥ 95%.The adsorption capacity (Q_e) and adsorption percentage ($\%Ads$) were calculated using equations 7 and 8 (Gani *et al*., 2023).

$$Q_e = \frac{(C_o - C_e)V}{m_B} \quad [7]$$

$$\%\, Ads = \frac{C_o - C_e}{C_o} \times 100 \quad [8]$$

With, Q_e being the apparent adsorption capacity or the equilibrium capacity of the biosorbent (mg g^{-1}), C_o the initial concentration of Rhodamine B solution (mg L^{-1}), C_e the residual or equilibrium concentration (mg L^{-1}), V the volume of Rhodamine B solution (L) and $\%Ads$, the adsorption percentage.

Adsorption kinetics

The modeling of the adsorption kinetic was done according to Lagergren kinetic model (Mekky *et al*., 2020; Ajala *et al*., 2024) using the kinetic equations of the surface reaction of pseudo-first-order and pseudo-second-order developed by Kifuani (Kifuani *et al*., 2012; Kifuani, 2013, Kifuani *et al*., 2018b):

Kifuani Pseudo-first- order kinetic model:

$$\ell n \frac{q_e}{(q_e - q_t)} = k_1 t \quad [9]$$

With, q_e being adsorption capacity at equilibrium (mg g^{-1}), q_t adsorption capacity at time t (mg g^{-1}), q_e-q_t adsorption capacity of free sites, t the time (s) and k_1, the constant rate of pseudo-first-order reaction (min^{-1}). The plot of $\ell n \frac{q_e}{(q_e - q_t)}$ versus t gives a line whose slope corresponds to k_1, the rate constant of pseudo-first-order reaction.

Kifuani Pseudo-second-order kinetic model:

$$\frac{q_t}{q_e(q_e - q_t)} = k_2 t \quad [10]$$

Where, k_2 is the rate constant of the pseudo- second- order reaction (g mg^{-1} min^{-1}). The plot of $\frac{q_t}{q_e(q_e - q_t)}$ versus t, gives a line whose slope corresponds to k_2, the rate constant of the pseudo-second–order reaction.

Adsorption isotherms

The modeling of the adsorption equilibrium was done using the Langmuir and Freundlich models given by the following equations 11, 12 and 13 (Mekhalef *et al*., 2018; Gani *et al*., 2023):

Langmuir model:

$$\frac{1}{Q_e} = \frac{1}{Q_m} + \frac{1}{Q_m K_L} \cdot \frac{1}{C_e} \quad [11]$$

Where, Q_e is the apparent adsorption capacity of the biosorbent (mg g^{-1}), Q_m the adsorption capacity at saturation or maximum adsorption capacity (mg g^{-1}), K_L equilibrium constant adsorption (L mg^{-1}) and Ce, equilibrium concentration. The plot of $1/Q_e$ versus $1/C_e$ gives a line which allows to determine Q_m and K_L, from the intercept and slope, respectively.

The Langmuir separation parameter (R_L) was calculated using equation 12 (Hajir *et al*., 2024):

$$R_L = \frac{1}{1 + K_L C_o} \quad [12]$$

With, K_L being the Langmuir constant (L mg^{-1}) and C_o the initial dye concentration.

Freundlich model:

$$\log Q_e = \log K_F + \frac{1}{n} \log C_e \quad [13]$$

Where, Q_e the adsorption capacity at equilibrium (mg g^{-1}), K_F the adsorption constant (Freundlich constant), C_e the concentration of the adsorbate at equilibrium (mg L^{-1}) and n, the Freundlich constant, characterizing the affinity of solute for the adsorbent (affinity parameter). The plot of log Q_e versus log C_e gives a line which allows to determine K_F and $1/n$ from the intercept and slope, respectively.

RESULTS

Characteristics of the biosorbent MPB

Table 1 presents the physicochemical characteristics of MPBbiosorbent. The maximum observed adsorption capacity (Q_{mo}) is 90.00 mg/g, with a specific surface area of 296.52m^2 g^{-1}(calculated with Q_{mo}, using methylene blue as adsorbate). The biosorbent is weakly acidic with pH_{ZPC} of 5.51.

Table 1. Physicochemical parameters of MPB

Parameters	Values
Humidity (%H)	5.38
Ash (%C)	4.40
Dry matter (%)	94,62
Particle size (µm)	≤ 0.50
pH_{ZPC}	5.51
Q_{mo} (mg. g^{-1})	90.00
Specific area, S_{BM} ($m^2.g^{-1}$)	296.52

Effect of biosorbent amount

Table 2, Figures 2 and 3 give theeffect of the amount of MP biosorbent on adsorption of RhB. The results obtained show that the maximum adsorption capacity of MPB decrease from 41.60mg/g to 3.79mg/g, when the amount of the biosorbent increases from 50 g to 1000 g (Table 2, Figure 2). In the other hand, the maximum adsorption capacity increases from 41.60% to 75.78%, when the mass of the biosorbent increase (Table 2, Figure 3). 800 mg of MPB were evaluated as the optimal adsorption weight of the adsorbent, with a %m*Ads* of 75.35% and Q_m of 4.71 mg/g, after 210 min. After this amount of biosorbent, the maximum adsorption capacity and the maximum adsorption percentage tend towards constants.

Table 2. Maximum adsorption capacity (Q_m), maximum percentage of adsorption (%$_m$*Ads*) and equilibrium time (t_e) at different weights of biosorbent (m_{MPB})

m_{BA}(mg)	Q_m (mg. g^{-1})	%$_m$*Ads*	t_e (min)
50	41.6	41.6	240
100	22.32	44.65	240
200	13.97	55.89	240
400	7.66	61.3	210
600	6.01	72.11	210
800	4.71	75.35	210
1000	3.79	75.78	190

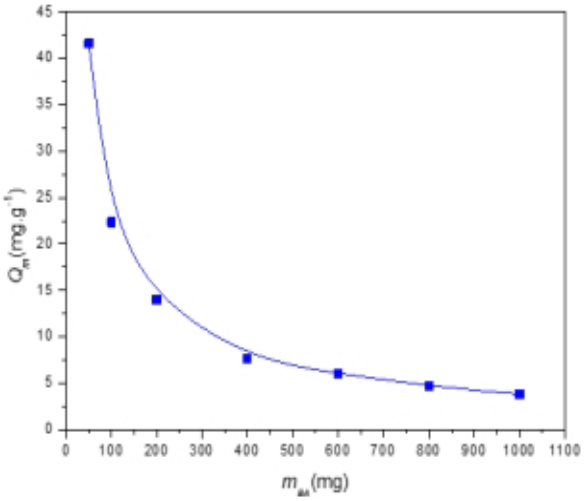

Figure 2. Maximum adsorption capacity (Q_m) vs dose of biosorbent (m_{BA})

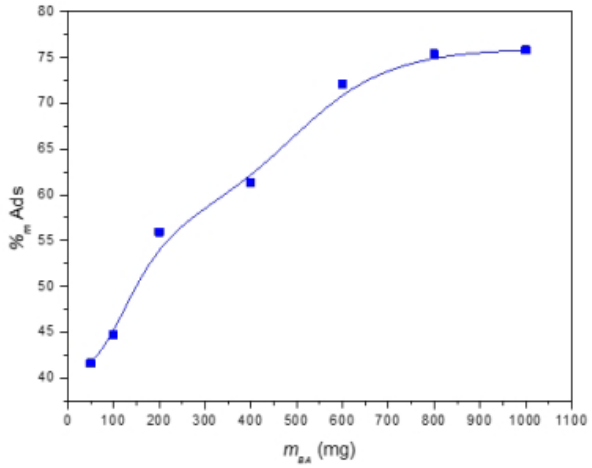

Figure 3. Maximum percentage of adsorption (%$_m$*Ads*)vs dose of biosorbent (m_{BA})

Effect of contact time

The results on the effect of contact time between MPB and RhB dye are presented in Figures 4 to 9, for different parameters studied (mass of biosorbent, initial concentration and pH of Rhodamine B dye solutions). From these results it appears that the adsorption capacity and the adsorption percentage of the biosorbent increase with MPB-RhB contact time. The optimum equilibrium time is estimated at 250 minutes for all parameters. The curves obtained by plotting the adsorption capacity or the adsorption percentage vs MPB-RhB contact time show three adsorption phases: a first rapid phase at the start of adsorption till 50 minutes, followed by a second slow phase (from 50 minutes to 250 minutes) and a third adsorption phase (from 250 minutes to 400 minutes) showing the achievement of the maximum apparent adsorption and the maximum apparent adsorption percentage. At this time, the adsorption is constant.

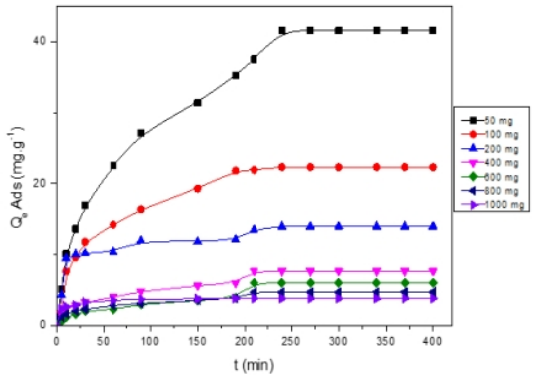

Figure 4. Effect of contact time (*t*) on adsorption capacity (Q_e) of MPB at different doses of biosorbent

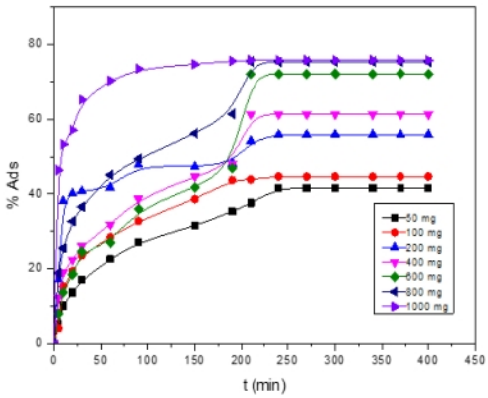

Figure 5. Effect of contact time (*t*) on the percentageadsorption (*% Ads*)of RhB on MPB at different doses of biosorbent

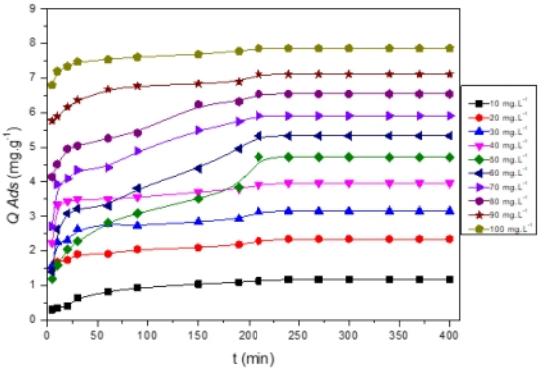

Figure 6. Effect of contact time (*t*) on the adsorption capacity *(Q_e)* of MPB at different initial concentrations of RhB solution

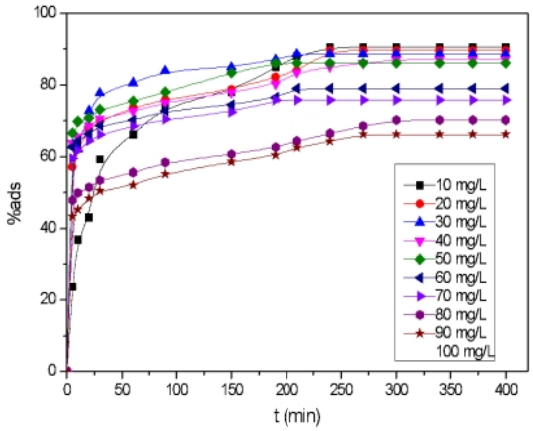

Figure 7. Effect of contact time (*t*) on the percentage of MPB adsorption (*% Ads*)at different initial concentrations of RhB solution

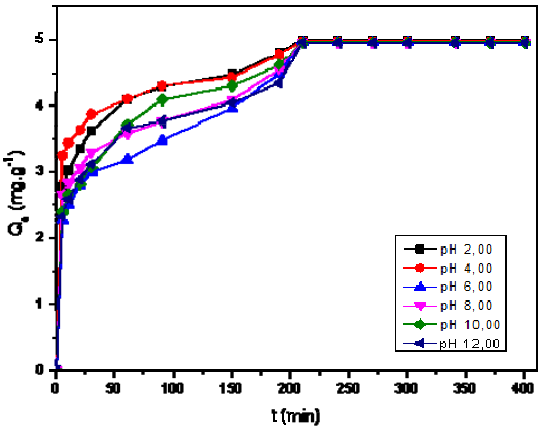

Figure 8. Effect of contact time (*t*) on the adsorption capacity of MPB (*Qe*)at different pH of RhB solution

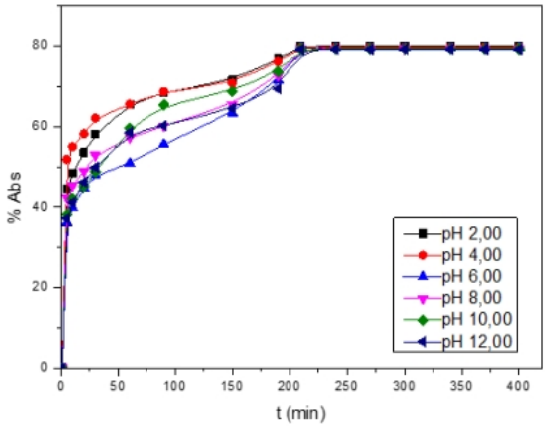

Figure 9. Effect of contact time (*t*) on the percentage of MPB adsorption (*% Ads*) at different pH of RhB solution

Effect of initial Rhodamine B dye concentration

The effect of the initial concentration of RhB on the adsorption is given by Figures 10 and 11. From Figure 10 it appears an increase in the maximum adsorption capacity from 1.17 mg/g to 7.11 mg/g when the initial concentration of Rhodamine solution increases; on the other hand, Figure 11 shows a decrease in the maximum adsorption percentage from 93.31% to 63.24%,with the increase in the initial concentration of RhB. The equilibrium time of adsorption decreases from 250 minutes to 210 minutes, when the concentration of Rhodamine dye increases from 10 mg L^{-1} to 100 mg L^{-1}.

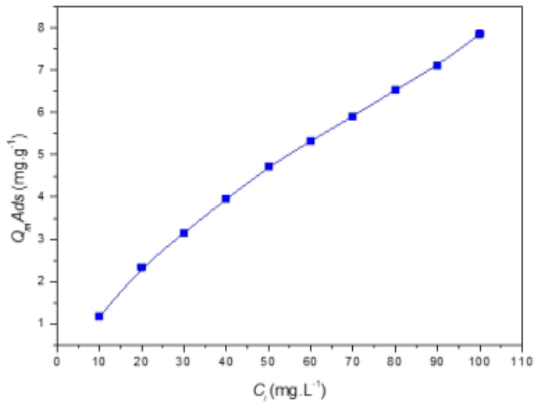

Figure 10. Effect of initial concentration (C_i) on themaximum adsorption capaciy (Q_m *Ads*) of MPB

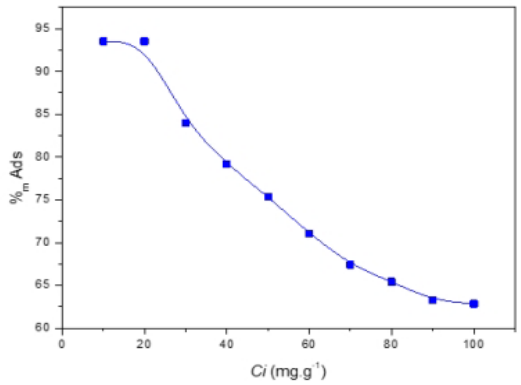

Figure 11. Effect of initial concentration (C_i) on the maximum adsorption percentage ($\%_m$ *Ads*) of MPB

Effect of pH

The effect of pH of the solution on the adsorption of Rhodamine B dye onto MPB biosorbent is given by Table 3 and Figure 12. From these results it appeared that the maximum adsorption capacity and maximum adsorption percent decrease slightly when the pH of the solution increases. The optimum maximum adsorption capacity and maximum adsorption percentage are evaluated at4.96 mg/g and 79.35%, at pH 8.00, after 210 minutes. A reduction of 0.94% is observed in the maximum adsorption percentage, when pH increases from 2 to 12.

Table 3. Maximum adsorption capacity (Q_m), maximum percentage of adsorption (*% Ads*) and equilibrium time (t_e) at different pH

pH	Q_{mo} (mg/g)	%*Ads*.	*te*
2.00	5.00	79.95	210
4.00	4.98	79.67	210
5.50	4.97	79.48	210
8.00	4.96	79.35	210
10.00	4.96	79.31	210
12.00	4.95	79.20	210

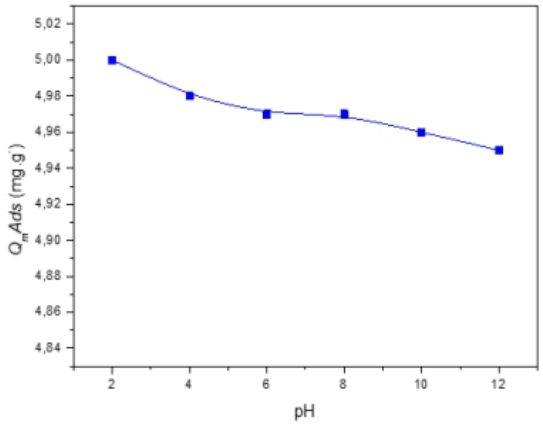

Figure 12. Effect of pH of RhB solution on maximum adsorption capacity (Q_m) of MPB

Modeling of adsorption kinetics

Kinetic data were analyzed using pseudo-first-order and pseudo-second-order models. The correlation coefficients (R^2g) obtained were 0.8975 and 0.9002, respectively (Table 4).

Modeling of adsorption isotherms

The adsorption isotherms of the adsorption of Rhodamine on MPB were modeled according to the two-parameters equilibrium models of Langmuir and Freundlich. The results obtained are summarized in table 5. The table gives the specific parameters of each model including Langmuir parameters (Q_m, K_L and R_L) and Freundlich parameters (K_F and $1/n$).The overall correlation coefficients (R^2_g) of Langmuir and Freundlich models are respectively 0,9049 and 0,9385.

Table 4. Pseudo-first order and pseudo-second order parameters for adsorption of RhB onto MPB at different pH

	Parameters of pseudo-first- order		Parameters of pseudo-second- order	
pH	k_1 (min^{-1})	R^2	k_2 (g.mg^{-1}min^{-1})	R^2
2.02	0.0089	0.9342	0.0122	0.8456
4.02	0.0076	0.9374	0.0088	0.8969
6,61	0.0148	0.8458	0.0254	0.9453
8.08	0.0124	0.9156	0.0274	0.8279
10.02	0.0119	0.8824	0.0122	0.9634
12.02	0.0082	0.8695	0.0078	0.9218
R^2_g		0.8975		0.9002

Table 5. Langmuir and Freundlich parameters for the adsorption of RhB onto MPB at different pH

pH	Q_m(mg/g)	Langmuir parameters			Freundlich parameters		
		K_L (L mg^{-1})	R_L	R^2	K_f (mg g^{-1}) (mg L^{-1})$^{-1/n}$	1/*n*	R^2
2.00	5.00	0.0744	0.2119	0.9379	0.8775	0.8774	0.9616
4.00	4.98	0.3428	0.0551	0.8779	1.1609	1.1608	0,8956
5.50	4.97	0.5869	0.0329	0.9559	1.6128	1.6127	0.9343
8.00	4.96	0.0272	0.4240	0.9110	1.5779	1.5779	0.9590
10.00	4.96	0.0356	0.3595	0.8019	0.5567	0.5567	0.9192
12.00	4.95	0.0014	0.9367	0.9445	0.7665	0.7665	0.9614
R^2_g 0.3367				0.9049	1.0920		0.9385

DISCUSSION

The maximum observed adsorption capacity (Q_{mo}) of MPB with a value of 90.00 mg g^{-1} (Table 1) is very high compared to that reported by Senol *et al*. (2024), with 14.70 mg g^{-1} for the adsorption of Rhodamine B dye by using a biosorbent from agricultural solid waste (almond shell).The surface of the biosorbent MPB is neutral at pH 5.51, which is thepH_{ZPC}; then, the surface of the biosorbent is positive at pH <pH_{ZPC}, and negative at pH>$pH_{ZPC.}$ The decrease in maximum adsorption capacity of MPB with increasing biosorbent mass is due to the biosorbent mass effect, resulting from steric hindrance (Table 2 and Figure 2). This phenomenon makes some active sites of the biosorbent inaccessible, but taken into account in the calculation of the adsorption capacity (Kifuani *et al*., 2018a). The observed increase in adsorption efficiency with rising biosorbent mass can be attributed to the enhanced availability of active surface sites, which facilitates greater interaction between the adsorbent and the target molecules(Table 2 and Figure 3).Similar results have also been reported by other researchers, confirming the positive correlation between biosorbent dosage and adsorption efficiency (Gani *et al*., 2023).

The progressive enhancement of both adsorption capacity and efficiency with time can be explained by the initial abundance of free active sites on the biosorbent surface. As the adsorption process proceeds, these sites become increasingly occupied, leading to a gradual saturation and a slower rate of adsorption.This explains the three phases of the curves (Figures 4 to 9). The horizontal part of the curve shows a total saturation of adsorption sites, and indicates that the maximum apparent adsorption capacity is reached (Kifuani *et al*., 2018a;Nigist *et al.,*2022; Gani *et al*., 2023; Ajala *et al*., 2024). The increase in adsorption capacity of MPB with rising initial concentration of Rhodamine B is attributed to the greater availability of free active sites at higher solute concentrations (Figures 10 and 11). An increase in solute concentration leads to a higher solute mass in the system, which in turn enhances the diffusion of solute particles (Fick's law). This phenomenon facilitates more frequent interactions between the solute and the biosorbent surface, thereby contributing to improved adsorption performance. Although the adsorption capacity tends to increase with higher initial concentrations, the percentage of adsorption generally decreases. This decline can be attributed to the saturation of available active sites on the biosorbent surface, which limits the proportion of solute that can be effectively adsorbed at elevated concentrations. A mass effect is observed. Musah *et al*. (2020) also reported the same observations on the decrease in the adsorption percentage with the concentration of the solution for the adsorption of methylene blue on a biosorbent from *Platanus orientalis* leaf powder.

The pH of the solution plays a critical role in regulating the surface charge distribution of the biosorbent. Variations in pH can alter the ionization state of functional groups on the biosorbent surface, thereby influencing its affinity for charged solute species and affecting the overall adsorption performance. The distribution of charges on the surface (S) of the biosorbent is as follows:

At pH < pH_{ZPC}: S-OH + H_3O^+ ↔ SO^+H_2 + H_2O
At pH= pH_{ZPC}: SO^+H_2↔ S-OH + H^+
At pH> pH_{ZPC}: S-OH + HO^- ↔ S-O^- + H_2O

At pH= pH_{ZPC} (=5.51), the surface of the MPB biosorbent is neutral. Below the pH_{ZPC}, the surface of the biosorbent is positively charged, and beyond pH_{ZPC}, the surface of the biosorbent is negatively charged. Adsorbate solution pH greatly influences adsorbate behavior. Rhodamine B exhibits different forms depending on the solution pH: lactonic at pH lower than 1.0, cationic at pH range 1 to 3, and zwitterionic at pH greater than 3.7. The tendency exhibited by the zwitterionic form of RhB leads to its dimer formation, thus reducing adsorption potential at pH above 4 (Folahan *et al*., 2019). As the pH of the rhodamine solution increases, its adsorption onto biosorbents decreases (Table 3, Figure 12); this mainly due to the reduced electrostatic attraction: at low pH (< 5.1), biosorbent surfaces are protonated and attract the cationic dye. At high pH (> 5.1), deprotonation leads to negatively charged surfaces, but excess hydroxide ions compete for binding sites and may hinder dye interaction. Additionally, rhodamine B may become more soluble or aggregate, further lowering its adsorption efficiency. This finding has also been independently observed by other researchers, supporting the robustness of the result (Folahan *et al*., 2019; Senol *at al*., 2024). The results obtained in this study indicate that the adsorption of Rhodamine B onto the biosorbent is only slightly influenced by pH. This suggests that the interaction mechanisms may not be predominantly governed by electrostatic forces, but rather by other factors such as hydrophobic interactions or specific functional groups present on the biosorbent surface. The optimum pH was estimated to be 5.50 with an optimum Q_m of 4.97 mg/g and optimum $\%_m Ads$ of 79.48% (Table 3, Figure 12).

The pseudo-first-order and pseudo-second-order models are suitable for describing the adsorption of Rh onto MPB, as the overall correlation coefficients obtained in both cases are close to unity (Table 4). Although both pseudo-first-order and pseudo-second-order models provide a good fit to the experimental data, the pseudo-second-order model (R^2_g 0.9002) proves to be more suitable for describing the adsorption of Rh onto MPB. This is evidenced by its higher correlation coefficient and better agreement with the observed adsorption kinetics, suggesting that chemisorption may be the rate-limiting step in the process. This correlation, less than 1, does not exclude other adsorption mechanisms. Similar kinetic results have been reported in the literature (Musah *et al.*, 2020).

Equilibrium data were fitted to both Langmuir and Freundlich isotherms. The Langmuir model yielded a correlation coefficient of 0.9049, while the Freundlich model produced a higher value of 0.9384 (Table 5). This indicates that the adsorption process is better described by the Freundlich model, implying heterogeneous surface adsorption and the possibility of multilayer coverage. Such behavior is consistent with the complex nature of biosorbent surfaces, which often contain a variety of functional groups and binding sites. The equilibrium parameter or separation parameter, K_L, indicates the affinity of the biosorbent towards rhodamine B, which can be favorable (0 <R_L<1), irreversible (R_L=0), linear (R_L =1) or unfavorable (R_L>1) (Hajir *et al*., 2024; Kifuani *et al*., 2024:). The K_F values represent the adsorbent power of the biosorbent, when the concentration (C_e) of RhB is unitary. The Freundlich parameter 1/*n* indicate the adsorption intensity or adsorption interaction strength. It is reported that the adsorption can be favorable (1/*n*<1), linear (1/*n* = 1), physical and unfavorable (1/*n*>1) (Bharath *et al*., 2022; Basma *et al*. 2024; Hajir *et al*. 2024).

The values of R_L less than 1 obtained for all pH studied, indicate that the adsorption of RhB on MPB biosorbent is favorable.

Conclusion

The eco-friendly biosorbent based on *Musa paradisiaca* was used for the removal of rhodamine B dye in aqueous solution. Adsorption were carried out in batch tests by varying several parameters. The experimental results demonstrate that biosorbent has a specific surface area of 296.52 m^2 g^{-1} and a maximum observed adsorption capacity (Q_{mo}) of 90.00 mg g^{-1}.the adsorption capacity was found to increase progressively with contact time across different biosorbent masses, initial dye concentrations, and pH levels. This time-dependent behavior confirms the gradual saturation of active sites, and supports the relevance of kinetic modeling to describe the adsorption mechanism. The experimental results demonstrate that the adsorption percentage decreases from 79.20% to 75.95% as the pH increases from 2 to 12. From this result, it appears that the adsorption process is only slightly influenced by pH, suggesting that electrostatic interactions are not the dominant mechanism. Instead, the adsorption appears to be governed by other factors such as hydrophobic interactions and the presence of specific functional groups on the biosorbent surface. Kinetic data were analyzed using pseudo-first-order and pseudo-second-order models. The correlation coefficients obtained were 0.8975 and 0.9002, respectively. Although both models show reasonable fit, the slightly higher Rg^2 value for the pseudo-second-order model suggests that chemisorption may play a more significant role in the adsorption process, involving valence forces through sharing or exchange of electrons between the dye molecules and the biosorbent surface. Equilibrium studies further supported these findings, with the Freundlich isotherm ($Rg^2 = 0.9384$) providing a better fit than the Langmuir model ($Rg^2 = 0.9049$). This suggests that the adsorption occurs on a heterogeneous surface with multilayer coverage, which is consistent with the complex nature of biosorbent materials. The results obtained in this study show that the eco-friendly biosorbent from *Musa paradisiaca*is effective for removal rhodamine B or other organic dyes from wastewaters.

Competing interests: The authors declare that they have no competing interests.

Authors' contributions: All authors contributed to data analysis and discussion of results.

Acknowledgements: The authors of the manuscript gratefully acknowledge Jerry IKELE KURAYUM and Kifline MILEBUDI KIFUANI family for the facilities provided to Professor Anatole KIA MAYEKO KIFUANI, during the final editing of this article in Aurora-Denver, Colorado, USA.

REFERENCES

Ajala, E.O., Aliyu, M.O., Ajala, M.A., Mamba, G., Ndana,A.M., Olatunde, T.S. 2024. Adsorption of lead and chromium ions from electroplating wastewater usingplantain stalk modified by amorphous alumina developed from waste cans. *Scientific reports*, 14 :6055. DOI : https://doi.org/10.1038/s41598-024-56183-2.

Ali, K., Javaid, U.J., Ali, Z., Zaghum, M.J. 2021. Biomassderived adsorbents for dye and heavy metal removal from wastewater. *Adsorption Science and Technology,* 2021:1-14. DOI:https://doi.org/10.1155/2021/9357509.

Achouri, M.E.L., Taibi, M. 2018. Removal of cationic dye methylene blue from aqueous solution by adsorption on fly ash-based geoplymer. *J. Mater. Envir. Sci.,* 9(1) :32-46. DOI : https://dx.doi.org/10.26872/jmes.2018.9.1.5.

Basma, G., Alhogbi, G. S., Al, B. 2023. An investigation of a natural biosorbent for removing methylene blue dye from aqueous solution. *Molecules*, 28 (6): 2785. DOI: https://doi.org/10.3390/molecules 28062785.

Bharath, B.G., Senthil, P. 2022. Adsorptive Removal of Alizarin Red S onto sulfuric acid modified avocado Seeds: Kinetics, Equilibrium, and Thermodynamic studies. *Adsorption Science & Technology,*2022 : ID3137870. DOI :https://doi.org/10.1155/2022/3137870.

Chadelaud, T., Zeghioud, H., Reynoso de la Garza, A., Fuerte, O., Bernitez-Rico, A., Revel, M., Chavez-Miyauchi T.E., Djelal H. 2023. Comparative study of rhodamine treatment: assessing of efficiency processes and ecotoxicity of by-products. *Processes* 2023, *11*(9), 2671. DOI: https://doi.org/ 10.3390/pr11092671.

Folahan,A.A., Suleiman, B.A, Adejumoke, A. I. 2019. Efficient rhodamine B removal using acid and alkaline-activated *Musa paradisiaca* biochar. *Pol. J. Environ. Stud*., 28(5): 3063-3070. DOI: https://dio.org/10.15244/pjoes/94386.

Gani, P., Puji, L. 2023. Comparison of two biosorbent beads for methylene blue discoloration in water. *J. Ecol. Eng.,* 24(8):137-145. DOI: https://doi.org/10.12911/22998993/166319.

Hajir, N., Abdelrahman, B.F., Omar, A.S. 2024. Isothermaland kinetics investigation of dibenzothiophene removal from model fuel by activated carbon developed from mixed date seed and PET Wastes. *Journal of Ecological Engineering,* 25(3): 38–52. DOI: https://doi.org/10.12911/ 22998993/177628.

Hatiya, N.A., Reshad, A.S., Negie, Z.W. 2022. Chemicalmodification of Neem (*Azadirachta indica*) biomass asbiosorbent for removal of Pb^{2+} ion from aqueous wastewater. *Adsorption Science and Technology,* 2022 :1-18. DOI: https://doi.org/10.1155/2022/7813513.

Jan, S.U., Ahmad, Y., Ali, M., Hussain, Z., Melhi, S. 2022.Adsorptive removal of methylene blue from aqueous solution using sawdust. *Medicom Pharmaceutical Sciences,* 2 (1): 8-16.

Jia, P., Tan, H., Liu, K., Gao, W. 2018. Removal of methylene blue from aqueous solution by bone char. *Appl. Sci.,* 1903: 1-11. DOI: 10.3390/app8101903.

Kifuani, A.K.M, Noki, P.V., Ndelo, J.D.P, Mukana, W.M., Ekoko, G.B., Ilinga, B.L., Mukinayi, J.M. 2012. Adsorptionde la quinine bichlorhydrate sur charbon actif peu couteux à base de la bagasse de canne à sucre imprégnée de l'acide phosphorique. *Int. J. Biol. Chem. Sci.,* 6(3): 1337-1359. DOI: dx.doi.org/10.4314/ijbcs. v6i3.36.

Kifuani, A.K.M. 2013. Adsorption des composés organiquesaromatiques en solution aqueuse sur charbon actif à basedes déchets agroindustriels. *Thèse de doctorat*, Université de Kinshasa.

Kifuani, K.M., Kifuani, A.K.M., Ilinga, B.L., Ngoy, P.B., Monama, T.O., Ekoko, G.B., Mbala,B.M., Muswema, J.LL. 2018a. Adsorption d'un colorant basique Bleu de Methylene en solution aqueuse sur un bioadsorbant issu de déchets agricoles de *Cucumeropsis mannii* Naudin. *Ind. J.*

Biol. Chem. Sci., 12 (1):558-575. DOI: https: //dx.doi.org/ 10.4314/ijbcs.v12i1.43.

Kifuani, K.M., Kifuani, A.K.M., Ilinga, B/L., Ngoy, P.B., Monama T.O., Ekoko, G.B., Muswema, J.L. 2018b. Kinetics and thermodynamic studies adsorption of Methylene Bleu in aqueous solution on a bioadsorbent from *Cucumeropsis mannii* Naudin waste seeds. *Int. J.Biol.Chem. Sci.,* 12 (5): 2412-2423. DOI: https: //dx.doi. org/10.4314/ijbcs.v12i5.38.

Kifuani, A.K.M., Mbenge, L., Kifuani K.M., Tshene, B. W., Tuluenga M., Zola.2024. Removal of basic organic dye methylene blue from aqueous solution by adsorption onto a low-costbiosorbent made from water hyacinth (*Eichhorniacrassipes*). *International Journal of Science Academic Research,* 05(12): 8728-8736. http :// www.scienceijsar.com

Mekhalef, B.F., Kacha, S.L.A., Belaid, K.D. 2018. Étude comparative de l'adsorption du colorant Victoria Bleu Basique à partir des solutions aqueuses sur du carton usagé et de la sciure de bois. Revue des sciences de l'eau /*Journal of Water Science,* 31(2): 109–126. DOI: https://doi.org/ 10.7202/1051695ar.

Mekky, A.E.M., El-Masry, M.M., Khalifa, R.E., Omer, A.M., Tamer, T.M., Khan, Z.A., Gouda, M., Mohy, Eldin, M.S. 2020. Removal of methylene blue dye from synthetic aqueous solutions using dimethylglyoxime modified amberlite IRA-420: kinetic, equilibrium and thermodynamic studies. *Desalination and Water Treatment*, 181: 399-411. DOI: 10.5004/dwt.2020.25097.

Musah, B.M., Peng, L., Xu, Y. 2020. Adsorption of methylene blue using chemically enhanced *Platanus orientalis* leaf powder: kinetics and mechanisms. *Nat. Env. &Poll. Tech*., 19 (1): 29-40. www.neptjournal.com.

Narayana, S.K.V., Ravi, V.K. 2019. Adsorption isotherm studies on methylene blue dye removal using naturally available biosorbent. *Rasayan J. Chem.,* 12(4): 2176- 2182. DOI: http://dx.doi.org/10.31788/RJC.2019.1245478.

Nigist, A.H., Ali, S.R., Zemene, W.N. 2022. Chemical modification of neem (Azadirachta indica) biomass as biosorbent for removal of Pb^{2+} ion from aqueous wastewater. Adsorption Science & Technology, 2022: 18. DOI: https://doi.org/10.1155/2022/7813513.

Nyakairu, G.W.A., Kapanga, P.M., Ntale, M.,Lusamba, S.N., Tshimanga, R.M., Ammari, A., Shehu, Z. 2024. Synthesis, characterization and application of Zeolite/Bi_2O_3 nanocomposite in removal of Rhodamine B dye from wastewater. *Cleaner Water*, 1(2024) :100004. DOI: https: //dx.doi.org/10.1016/j.clwat.2024.100004.

Pathania, D., Sharma, S., Singh, P. 2017. Removal of methylene blue by adsorption onto activated carbon developed from Ficus carica bast. *Arabian journal of chemistry*, 10: S1445-S1451. DOI:https: //dx.doi.org/ 10.1016/j.arabjc.2013.04.021.

Raiyyaan, G.D., Khalith, M. S.B., Sheriff, A.M., Arunachalam, K.D.A. 2021. Bio-adsorption of methylene blue dye using chitosan-extracted from *Fenneropenaeus indicus* shrimp shell waste, *J. Aquac. Mar. Biol.,* 10 (4): 146-150. https://medcraveonline.com.

Razia, S., Syed, N.T., Usman, T.S., Yunus, K.T.M., Shaik,D.A.K., Imran, M., Kiran, S., Kalam, M.A., Ananda, M.H.C., Akheel, A.S. 2022, Adsorption of Crystal Violet dye from aqueous solution using industrial pepper seed spent: Equilibrium, Thermodynamic, and Kinetic Studies. *Adsorption Science & Technology.,* 2022:ID9009214. DOI: https://doi.org/10.1155/2022/9009214.

Senol, Z.M., Messoudi, N.E., Fernine, Y., Keskin, Z.S. 2024. Bioremoval of rhodamine B dye from aqueous solution by using agricultural solid waste (almond shell):experimental and DFT modeling studies. *Biomass Conv. Bioref*., 14, 17927-17940. DOI: https://doi.org/10.1007/s 13399-023-03781-1.

Tshene, B.W., Kifuani, K.M., Kifuani, A.K.M., Ngoy, P.B., and Ekoko, G. B. 2024. Adsorption of a basic dye methylene blue in aqueous solution on a biosorbent from agricultural waste of Manihot esculanta Crantz. *Int. J. Biol.Chem. Sci.,* 18(3): 1180-1198. DOI: https://dx.doi.org/ 10.4314/ijbcs. v 18i3. 35.

****